THz direct detector with 2D electron gas periodic structure absorber.

D. Morozov[a], P. Mauskopf[a], I. Bacchus[a], M. Elliott[a], C. Dunscombe[a], M. Hopkinson[b], M. Henini[c]
[a]School of Physics and Astronomy, Cardiff University, 5 The Parade, CF24 3AA, UK
[b]Department of Electronics and Electrical Engineering, University of Sheffield, S10 2TN, UK
[c]School of Physics and Astronomy, University of Nottingham, NG7 2RD, UK

ABSTRACT

We describe the performance of a direct detector that uses the high mobility 2D electron gas (2DEG) formed at the AlGaAs/GaAs interface as a frequency selective absorber. The 2DEG mesa-structure is etched to form a planar periodic structure with resonant absorption properties in the submm - THz region. Electrons in the 2DEG are heated by incoming radiation above the lattice temperature and the temperature of the hot electrons is measured by Superconducting - 2DEG - Superconducting (S-2DEG-S) tunnel junctions. The estimated noise equivalent power for such a detector at 100 *mK* is in order of 10^{-18} $W/Hz^{1/2}$. In this paper we present the spectral measurements and simulated results of absorption properties at 4.2 *K* for a resonant mesa geometry. The thermal conductance and time constant of 2D electrons are studied at 450 *mK*-4.2 *K*. We measure an electron-phonon conductance on the order of 10^{-17} *W/K* per electron at 450 *mK* which gives a low value of heat conductance 2DEG relative to normal metal absorbers due to the low 2DEG electron density. These devices have a combination of sensitivity and speed which makes them possible candidates for the components in future astrophysical THz instruments.

1. INTRODUCTION

The development of high sensitivity direct detectors for mm-Thz radio-astronomy has been a field of active interest for a few decades. Transition Edge Sensors (TES) [1], normal metal - insulator - superconducor tunnel junctions (NIS) [2, 3] and cold electron bolometers (CEB) [4, 5, 6, 7] are some of the technologies which have achieved extremely low value of *NEP*. Microbolometers like NIS and CEB detectors make use of the thermal isolation between electrons and phonons in normal metal absorbers with submicron dimensions to detect THz radiation. The two-dimensional electron gas in AlGaAs/GaAs heterojunctions at 4.2 *K* and lower temperatures is weakly coupled to the lattice and the hot electron effect in the 2DEG can also be used to make a sensitive bolometric detector in THz range. The 2DEG electron mobility (μ) and density (n_s) can be set at optimal values during the semiconductor heterostructure's growth process so that a 2DEG will have up to 10^5 times lower thermal conductivity per unit area than a normal metal absorber with the same DC resistance. The lower thermal conductivity allows detector designs of greater than sub-micron size, facilitating construction. These advantages make 2DEG detectors good candidates for filled arrays of ultra-sensitive bolometers with free-space absorbers.

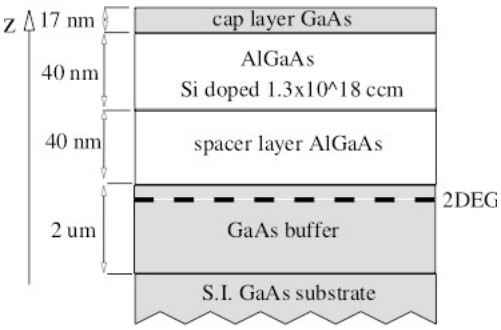

Figure 1: Heterostructure

In this paper we present low temperature transport measurements of 2DEG properties (thermal and electrical) and the design and measurements of a periodic absorber structure. We incorporate this absorber into a simple 2DEG HEB where the electron temperature is determined from the DC resistance of the 2DEG. We measure the sensitivity of this device at 4.2 K and compare it with estimates from DC IV curves. The sensitivity of the 2DEG HEB is limited by the slope of the resistance vs. temperature curve for the 2DEG. Finally we analyze a proposed detector consisting of a 2DEG as a radiation absorber and S-2DEG tunneling contacts as a thermometer to measure electron temperature of the 2D electrons.

2. SAMPLES AND EXPERIMENTAL TECHNIQUES

The heterostructures were grown by molecular - beam epitaxy and have the layer structure shown in fig. 1. We primarily used material from two growth runs, one from Nottingham University (NU03) and one from the University of Sheffield (S8).

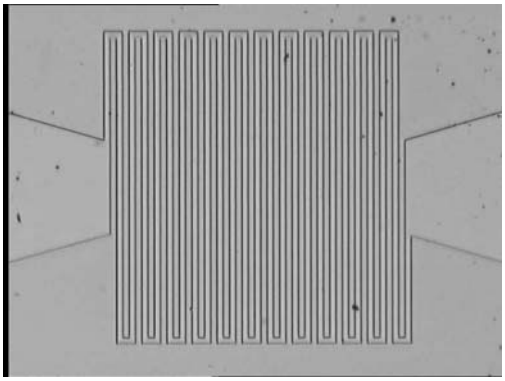

Figure 2: Optical microscope picture of the meander type detector.

The fabrication process for the devices included the following steps. First, mesas were formed by wet etching with $H_2SO_4/H_2O_2/H_2O$ etch solution. Then ohmic contacts were deposited by thermal evaporation of AuGe-Ni-Au and patterned in a "lift-off" process followed by thermal annealing in a N_2 gas atmosphere at $\approx 400^oC$ for 1 minute. We fabricated a variety of mesa geometries from the heterostructure wafer material. Hall bar devices were used to measure the thermal and electrical properties of the 2DEG. The mobility and electron density of 2D electrons at 4.2 *K* were found by measuring of Shubnikov-de-Haas oscillations period and amplitude with constant applied electrical power. For the heterostructures used in this study we measured μ =1.6 x 10^6 cm^2/Vs and n_s = 1.8 10^{11} cm^{-2}.

The absorber/detector design consisted of a meander geometry with ohmic contacts at either end. The path of the meander was 20 μm wide with a filling factor of 50%. It covered an area of 1x1 mm^2 and is shown in fig. 2. For optical tests of HEB detector with the meander absorber we used a simple setup with a blackbody radiation source with temperature T_{bb} = 800 *K*. The detector was mounted in an integrating cavity behind a Winston horn and thermally mounted on the cold stage of an cryostat at the base temperature close to 4.2 *K*. To block 300 K thermal radiation low-pass mesh filters with cut-off frequencies of ≈ 9 *THz* were placed at the 4 *K* and 77 *K* stages. The detector block with the horn inside the cryostat is shown in fig. 3. The power from the blackbody source was estimated to be $P_s \approx 3.1$ *nW* in the bandwidth of the filter in front of the detector. For the spectral measurements, the detector was placed at the output of a scanning Fourier Transform Spectrometer.

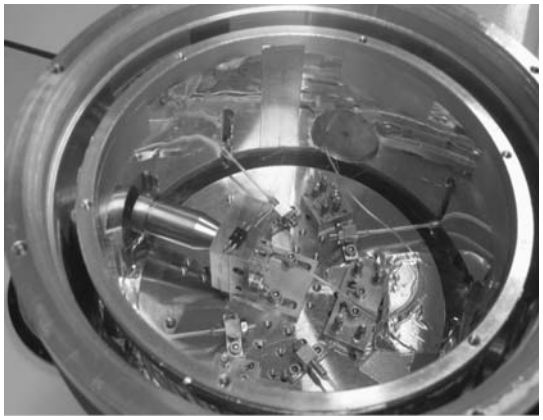

Figure 3:Picture of the detector block with Winston horn inside the cryostat.

3. EXPERIMENT AND DISCUSSION

We characterized the electrical and thermal properties of the 2DEG meander from the *R*(*T*) and using *IV* curves measured at different base temperatures. We obtained values for $(1/R)dR/dT$ and G_{th} at 4.2 *K* and 450 *mK* in agreement with the values measured in the Hall bars. These parameters are listed in table 1.

Optical tests of the meander-type detector gave us the results shown in fig. 4. The maximum value of $S_V \approx 233 V/W$ occurred at bias current $I_b = 10 \mu A$ and $NEP \approx 8.9 \times 10^{-11} W/Hz^{1/2}$. An electical *NEP* can be calculated from DC measurements using $S_V = I_b(dR/dT)/G_{th}$ and taking into account that noise has contribution from Johnson and phonon noise [8]. Calculated values were $S_V \approx 270 V/W$ and $NEP \approx 3 \times 10^{-11} W/Hz^{1/2}$. This indicates that the peak optical efficiency of the detector is about 30%. The time constant of the detector (τ) is estimated using a calculated value for the heat capacity of the electrons C_e and the measured G_{th} as $\tau = C_e/G_{th}$. To show the predicted performance of the same detector operated at *T*=450 *mK* we estimate the responsivity, *NEP* and time constant using the DC electrical characterisation. Experimental and theoretical data for different detector temperatures is given in table 2.

Table 1:Experimental data of the DC electrical and thermal transport.

Sample	$(1/R)dR/dT$ K^{-1} per square 4.2 *K*	$(1/R)dR/dT$, K^{-1} per square 450 *mK*	G_{th} , *W/K* 4.2 *K*	G_{th} , *W/K* 450 *mK*
NU03	75.2×10^{-3}	3.2×10^{-3}	1.5×10^{-15}	1.1×10^{-17}
S8	46.9×10^{-3}	3.1×10^{-3}	4.14×10^{-14}	1.2×10^{-16}

Table 2:Meander detector performance DC biased at I_b = 10 μA

T, K	S_V, *V/W*	*NEP, W/Hz$^{1/2}$*	τ, *ns*
experim. 4.2 *K*	233	8.9 x 10^{-11}	0.94
model 4.2 *K*	270	3 x 10^{-11}	≈1
model 450 *mK*	6 x 10^{3}	2.5 x 10^{-14}	≈100

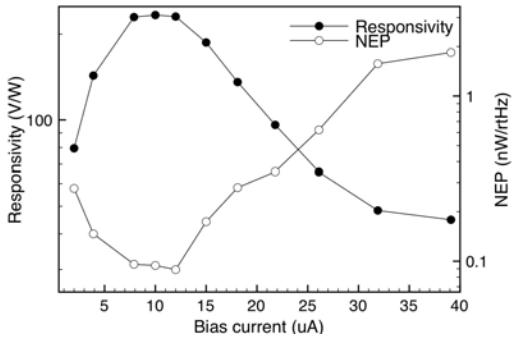

Figure 4:Responsivity and NEP for the meander type HEB detector.

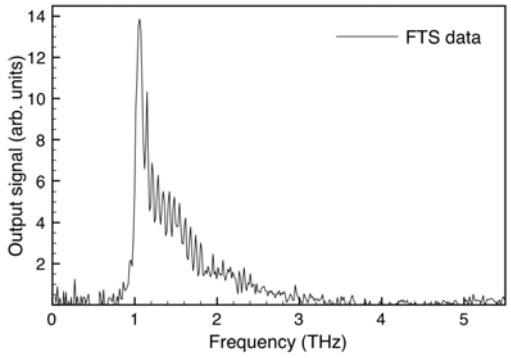

Figure 5: FTS spectrum of the meander detector.

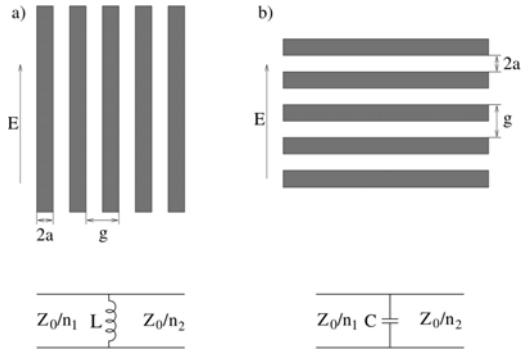

Figure 6:(a) Inducive and (b) capacitive strip periodic structures and their equivalent electric circuits.

Spectral measurements of the detector response have been made using a Fourier Transform spectrometer. The maximum detector response was in a narrow frequency range close to 1 *THz*. The dependance of the detector output signal on the frequency of the incident radiation is shown in fig. 5. The selectivity of the input signal frequency can be explained in terms of resonant absorption in periodic grid structures [9, 10]. Let us briefly discuss the model behind the resonance properties of periodic grid structures. The basic structures include inductive and capacitive gratings and they are shown on fig. 5 as well as corresponding equivalent circuits. The reactance of an inductive grid will be [9]:

$$\frac{X_l}{Z_0} = \frac{g}{\lambda} \ln \csc \frac{\pi a}{g}, \qquad (1)$$

where Z_0 = 377 Ohm is the free space impedance, λ is the free space wavelength. Similarily, the reactance of a capacitive grid will be:

$$\frac{X_c}{Z_0} = \frac{-2}{n_1^2 - n_2^2} \left(\frac{4g}{\lambda} \ln \csc \frac{\pi a}{g} \right)^{-1}, \qquad (2)$$

where n_1 and n_2 are dielectrics refractive indices. Here we assume the equivalent electric circuit with capacitance and inductance in series. For a real structure one should also include resistance R_0 in the above model (see fig. 7). The transmittance through the shunted circuit is given by [9]:

$$T = \frac{4 n_1 n_2 \left((R_0 / Z_0)^2 + (X / Z_0)^2 \right)}{\left(1 + (n_1 + n_2) R_0 / Z_0\right)^2 + (n_1 + n_2)^2 (X / Z_0)^2}, \quad (3)$$

here, $X = X_l + X_c$ is the full reactance of the circuit shown on fig. 7. In general this circuit will have a resonant absorption feature at a wavelength close to the periodicity of the structure $\lambda_0 \approx g$ in free space $n_1 = n_2 = 1$. But in the case of a 2DEG situated close to the surface of a GaAs with ε =12.9 the absorption resonance will shift to longer wavelengths $\lambda \approx 300\ \mu m$. Using equations (1), (2) and circuit simulator we obtained absorption spectrum shown in fig. 8 for radiation at normal incidence to the device. The projected pattern from the meander will appear smaller at larger incidence angles thereby spreading the resonant absorption towards higher frequencies.

A high performance detector based on a high mobility 2DEG requires the separation of the 2DEG absorber and the electron temperature thermometer. Using the 2DEG resistance as an indicator of the electron temperature [11, 12] limits both the

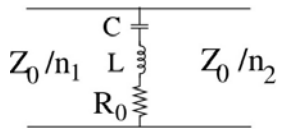

Figure7:Equivalent circuit for meander type detector

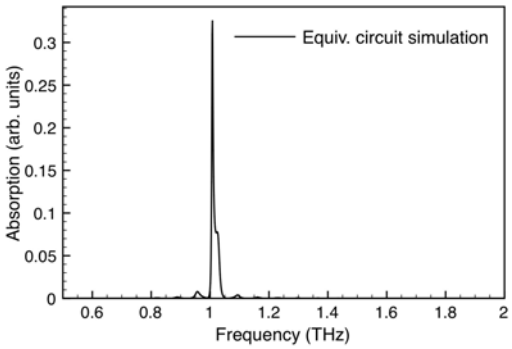

Figure 8: Simulated absorption spectrum

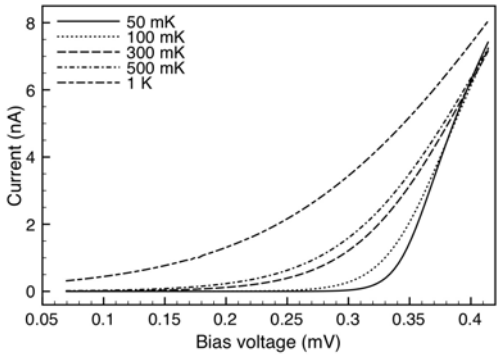

Figure 9: Computed I-V curves for the detector with two S-2DEG-S junctions at different temperatures

responsivity and the *NEP* due to weak $R(T)$ dependence of the 2DEG at liquid ^{4}He temperatures. A 2DEG detector with a higher dR/dT_e would have the advantages of both a low G_{th} absorber and high responsivity thermometer. We propose to use a 2DEG-Superconductor junction as a thermometer to read out T_e similar to Rowell and Tsui [13]. Tunnel junctions could be made by forming Schottky barriers in the interface between GaAs and superconducting contacts. We simulated a detector which has a 2DEG as a radiation absorber and two aluminum superconducting contacts with tunnel barriers as a thermometer. According to [2, 3] the tunneling current through the contact is given by:

$$I = \frac{1}{2eR_N}\int_{\Delta}^{\infty}\frac{1}{e^{(E-eV)/k_BT_e}+1}\frac{E}{\sqrt{E^2-\Delta^2}}dE, \quad (4)$$

where R_N is the normal state resistance of the junction, Δ is the energy gap of the superconductor and V is the bias voltage. For $(\Delta - eV) > k_BT$ the above equation simplifies to:

$$I \approx I_0 e^{-(\Delta-eV)/k_BT} \quad (5)$$

with $I_0 = (2eR_N)^{-1}\sqrt{2\pi\Delta k_BT}$. The junction can be current-biased such that the temperature responsivity dV/dT is $\approx -(k_B/e)\ln(I_0/I)$ [2, 3].

Calculated IV curves for different temperatures are shown in fig. 9. Values of R_N =5 *kOhm* and $2\Delta(0)_{Al}$ = 0.348 *meV* have been used [14]. Using the computed IV curves we estimate the detector performance. The assumed area of the absorber is 60 μm^2 and the operating temperature T = 100 *mK*. At bias current I_b = 0.4 *nA* the voltage response is $dV/dT \approx 287\ \mu V/K$, $S_V \approx 5.7 \times 10^9$ *V/W* and *NEP* $\approx 1.5 \times 10^{-18}$ *W/Hz*$^{1/2}$. For the estimation of *NEP* shot noise, Johnson noise and phonon noise contributions have been taken into account. In this type of detector at 100 *mK* shot noise contribution is dominant.

4. CONCLUSION

We report the experimental results of spectral measurements of a 2DEG absorber, electrical and thermal properties of the 2DEG at low temperatures. We also have measured performance of a 2DEG HEB as a direct detector of THz radiation at 4.2 *K*. We model the coupling of THz radiation to the 2DEG using a quasi-optical theory of periodic structures. This model reproduces the observed spectral response but it does not take into account the contribution of the kinetic inductance in the 2DEG as part of the equivalent circuit. Using these results, we estimate the *NEP* of a detector consisting of a 2DEG absorber and S-2DEG thermometer operating at 100 *mK* to be in order of 10^{-18} *W/Hz*$^{1/2}$.

This work is supported by a rolling grant from the Particle Physics and Astronomy Research Council (PPARC).

REFERENCES

[1] J. Zmuidzinas and P. Richards, "Superconducting detectors and mixers for millimeter and submillimeter astrophysics," *Proceedings of the IEEE* **92**, pp. 1597–1616, October 2004.

[2] M. Nahum and J. M. Martinis, "Ultrasensitive-hot-electron microbolometer," *Appl. Phys. Lett.* **63**, pp. 3075–3077, 1993.

[3] M. Nahum, T. M. Eiles, and J. M. Martinis, "Electronic microrefrigerator based on a normal-superconductor tunnel junction," *Appl. Phys. Lett.* **65**, pp. 3123–3125, 1994.

[4] D. Golubev and L. Kuzmin, "Non-equilibrium theory of a hot electron bolometer with normal metal-insulator-superconductor tunnel junction," *Jour. App. Phys.* **89**, pp. 6464–6472, 2001.

[5] L. Kuzmin and D. Golubev, "On the concept of an optimal hot-electron bolometer with nis tunnel junctions," *Physica C* **372-376**, pp. 378–382, 2002.

[6] L. Kuzmin, "Superconducting cold electron bolometer with proximity traps," *Micro. Elect. Engn.* **69**, pp. 309–316, 2003.

[7] D.-V. Anghel and L. Kuzmin, "Capacitively coupled hot-electron nanobolometer as far-infrared photon counter," *Appl. Phys. Lett.* **82**, pp. 293–295, January 2003.

[8] P. L. Richards, "Bolometers for infrared and millimeter waves," *Jour. App. Phys.* **76**, pp. 1–24, July 1994.

[9] L. B. Whitbourn and R. C. Compton, "Equivalent-circuit formulas for metal grid reflectors at a dielectric boundary," *Applied Optics* **24**(2), pp. 217 – 220, 1985.

[10] R. Ulrich, "Far-infrared properties of metallic mesh and its complementary structure," *Infrared Physics* **7**, p. 65, 1967.

[11] J. X. Yang, P. Agahi, D. Dai, C. F. Musante, W. Grammer, K. M. Lau, and K. S. Yngvesson, "Wide-bandwidth electron bolometric mixers: a 2DEG prototype and potential for low-noise THz receivers," *IEEE Trans. on Micr. Theo. and Techn.* **41**, pp. 581–589, 1993.

[12] J. X. Yang, J. Li, C. F. Musante, and K. S. Yngvesson, "Microwave mixing and noise in the two-dimensional electron gas medium at low temperatures," *Appl. Phys. Lett.* **66**, pp. 1983–1985, 1995.

[13] J. M. Rowell and D. C. Tsui, "Hot electron temperature in InAs measured by tunneling," *Phys. Rev. B* **14**, pp. 2456–2463, 1976.

[14] D. Morozov, I. Bacchus, P. Mauskopf, M. Elliott, C. Dunscombe, M. Henini, and M. Hopkinson, "High sensitivity terahertz detector using two-dimensional electron gas absorber and tunnel junction contacts as a thermometer," *Proc. SPIE* **6275**, p. 62751P, 2006.